

A Low-Cost Miniaturized Flower-Shaped Printed Antenna with Enhanced Bandwidth for UWB Applications

Nella Anveshkumar¹, Jai Mangal¹, Sudipta Das^{2, *},
Boddapati Taraka Phani Madhav³, and Wael Abd Ellatif Ali⁴

Abstract—This paper reports a novel, cost effective, and compact ultra-wideband (UWB) antenna for applications in an unlicensed-frequency band of 3.1–10.6 GHz. To achieve the UWB operation, a novel concept of annular shapes, circular slot combinations, and partial ground is employed. Furthermore, the proposed antenna with novel configuration occupies an attractive size of only $18 \times 12 \text{ mm}^2$ which allows compatibility with portable UWB application devices. This flower-horn shaped UWB antenna is printed on a cost-effective FR-4 substrate, which exhibits a dielectric-constant of 4.4 and a loss-tangent of 0.019. The fabricated prototype is experimentally tested, and measured results validate the design approach of presented UWB antenna. The measured results confirm its UWB characteristics covering 3.1–11.2 GHz with $S_{11} \leq -10 \text{ dB}$. Also, a maximum peak-gain of 5.05 dBi at 9 GHz and a minimum radiation-efficiency of 94.35% are noted in the full operating-band. A good agreement has been obtained between the simulated and measured results in terms of reflection-coefficient, gain, radiation-efficiency, radiation patterns, and group delay which confirm the suitability of suggested small printed antenna for the intended UWB applications.

1. INTRODUCTION

In today's wireless communication systems, ultra-wideband (UWB) technology is very attractive and a promising innovation due to its high bandwidth and data rate. UWB technology has gained strength when FCC (Federal Communications Commission) provided 3.1–10.6 GHz for unlicensed purpose in 2002 [1]. UWB technology can obtain a maximum data rate up to Gbps at distances from 1 to 10 meters. Example: for Bluetooth technology, a maximum data rate up to 1 Mbps is achieved for distances to 10 meters. Similarly, for GSM technology, a maximum data rate up to 100 Kbps is achieved for distances to 10 km or above.

UWB technology allows great flexibility to optimize the system performance by varying different parameters like data rate, range, power, and quality of service. A single system can offer wireless communication services for multiple applications without using additional hardware. Example: For short distance applications, low power and high data rate can be achieved. The UWB signals are transmitted with low power levels below a noise floor in which the quality of communication is also maintained. These signals are almost invisible to the other wireless operating signals. Hence, interference problem with other services can be avoided. This low power feature also helps the UWB systems in achieving a longer battery life. The UWB systems provide reliable and secure communications. Since the UWB signals are operated in low powers below a noise floor, they are very difficult to detect. The noise

Received 17 March 2022, Accepted 6 June 2022, Scheduled 21 June 2022

* Corresponding author: Sudipta Das (sudipta.das1985@gmail.com).

¹ School of EEE, VIT Bhopal University, Bhopal, India. ² Department of ECE, IMPS College of Engineering & Technology, Malda, West Bengal, India. ³ Department of ECE, Koneru Lakshmaiah Education Foundation, Andhra Pradesh, India. ⁴ Department of ECE, College of Engineering and Technology, Arab Academy for Science, Technology and Maritime Transport (AASTMT), Alexandria, Egypt.

signals also cannot eliminate the UWB signals completely. Because, the UWB signals have particular shape whereas the noise has no shape. Moreover, the noise has to interfere with the UWB signals uniformly throughout the spectrum. Even though the UWB signals can be recovered the noise interferes with them. Thus, the UWB signals are very strong in helping reliable and secure communications. The UWB signals are needed not to be modulated and demodulated (no up conversion and down conversion). Hence, the UWB systems do not require modules like mixers, additional oscillators, amplifiers, filters, etc. This advantage helps in reducing the cost, complexity, and size of the devices. Moreover, various modulation schemes like PAM, PPM, and phase shift keying can also be implemented using these small narrow pulses.

In wireless communication systems, planar antennas are very much compatible with portable devices. They achieve UWB performance by using different antenna structures [2–24]. A U-shaped microstrip-patch antenna [2] with novel parasitic-tuning stubs, having dimensions $24\text{ mm} \times 28\text{ mm} \times 0.787\text{ mm}$, is proposed for UWB applications. It provides a bandwidth ranging from 2.76 GHz to 12.8 GHz and achieves a maximum peak-gain of 5.3 dBi at 10.2 GHz. A CPW-fed compact UWB microstrip antenna with dimensions $25\text{ mm} \times 25\text{ mm} \times 1.6\text{ mm}$ is proposed [3]. It provides a bandwidth that ranges from 2.6 GHz to 13.04 GHz and achieves a maximum peak-gain of 4.25 dBi at 11.78 GHz. In paper [5], the authors proposed a planar monopole UWB antenna having dimensions $25\text{ mm} \times 20\text{ mm} \times 1.6\text{ mm}$. It provides a bandwidth ranging from 3.1 GHz to 10.64 GHz and achieves a maximum peak-gain of 4.34 dBi at 10.6 GHz. In paper [8], the authors proposed a UWB antenna having dimensions $35\text{ mm} \times 35\text{ mm} \times 1.6\text{ mm}$. It provides a bandwidth ranging from 3.1 GHz to 12 GHz and achieves a maximum peak-gain of 4.5 dBi at 10.6 GHz. A compact low-profile CPW-fed antenna [16] of dimensions $18.7\text{ mm} \times 17.6\text{ mm} \times 1.5\text{ mm}$, operating between 2.9 and 13.7 GHz is proposed for UWB applications. An average gain of 4.4 dBi and WLAN band rejection are achieved using slot insertion technique. A planar antenna of dimensions $12\text{ mm} \times 19\text{ mm} \times 1.6\text{ mm}$, operating in a band of 2.9–12 GHz is reported in [17] for FCC UWB applications. A peak-gain of 3.18 dBi and a maximum radiation efficiency of 95% are achieved.

Refs. [2–24] present several planar conventional type UWB antennas with good performance. However, compactness is a challenging task while UWB antennas are designed without degradation in the performance characteristics. The design challenges in a UWB antenna are compact size, stable UWB characteristics with good frequency, and time domain performance. In this proposed research study, a planar monopole antenna is reported in the frequency range of 3.1–10.6 GHz for UWB applications. This study also introduces a novel concept of annular shapes, circular slot combinations, and partial ground, which helps in achieving the wide operating-range of frequencies. The proposed antenna achieves a fractional bandwidth about 113.28 % (3.1–11.2 GHz) with a center frequency of 7.15 GHz by using a flower-horn structure over the substrate. A maximum peak gain of 5.05 dBi at 9 GHz and minimum radiation efficiency of 94.5% in the entire operating band are recorded for the designed antenna. This antenna exhibits compactness, stable wide band characteristics, and good performance compared with literature study. Hence, it is suitable for numerous UWB applications like W-BAN, W-LAN, cognitive radio (CR) spectrum sensing, wireless-sensor networks, etc. Moreover, the structure is unique, and the design techniques are novel. Rest of the paper is organized as follows. Section 2 presents a discussion on the proposed antenna configuration. Section 3 reports the design analysis of the proposed structure. Parametric analysis is reported in Section 4. Results and discussions are presented in Section 5. Conclusion is made in Section 6.

2. PROPOSED ANTENNA DESIGN

This section discusses the design of proposed compact monopole antenna with the combination of circular patches and slots. The dimensions of this antenna are $18\text{ mm} \times 12\text{ mm} \times 1.6\text{ mm}$. In the top view as shown in Fig. 1, the structure consists of a flower horn patch formed by placing six circular patches. A rectangular slot is positioned on the upper circle. Also, the concept of a partial ground is employed for designing the structure. The dimensions of the ground plane are $3\text{ mm} \times 12\text{ mm} \times 0.035\text{ mm}$. The ground plane has been modified by incorporating two rectangular slots and three circular slots to obtain the reflection coefficient below -10 dB for a wide range of frequencies. Dimensions of the antenna and performance characteristics are shown in Table 1

Table 1. Antenna parameters.

Parameter	Dimensions
Substrate	18 mm × 12 mm × 1.6 mm
Operating range	3.1 GHz to 11 GHz
Peak Gain	5.05 dBi at 9 GHz
Polarization	Linear

Top and bottom views of the proposed UWB antenna are shown in Fig. 1. Note that all dimensions are in mm. Simulated reflection coefficient curve of the proposed antenna is shown in Fig. 2.

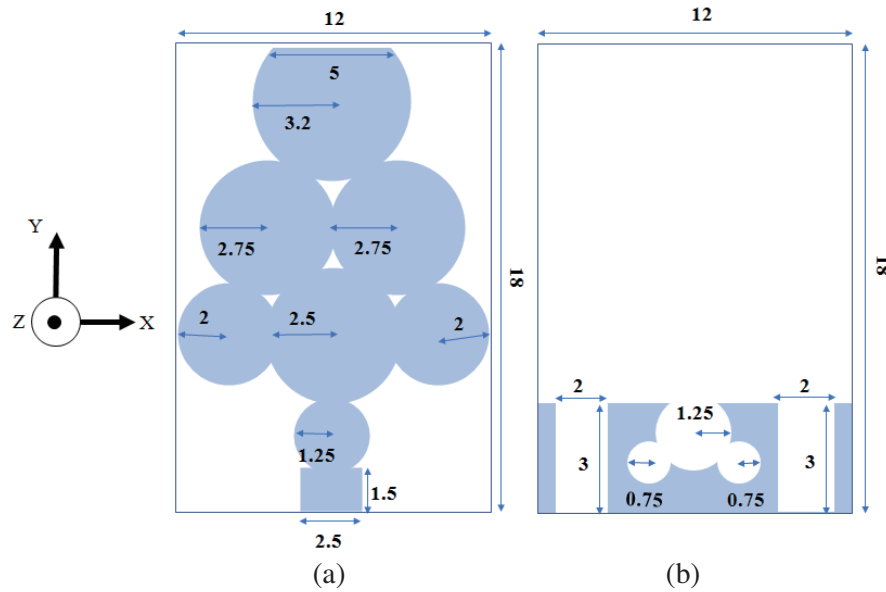


Figure 1. Proposed UWB antenna. (a) Top view. (b) Bottom view.

It can be observed from Fig. 2 that the proposed antenna attains a reflection coefficient below -10 dB over an unlicensed UWB frequency range, i.e., from 3.1 GHz to 11 GHz with two small resonating dips at 3.8 GHz and 9.9 GHz.

3. DESIGN ANALYSIS OF PROPOSED ANTENNA

This section reports design evolution of the proposed antenna by following various design steps. Initially, it discusses design analysis of the radiating patch and then followed by ground patch.

3.1. Design Analysis of Radiating Patch

The proposed structure as shown in Fig. 1 is the subsequent structure of an antenna as shown in Fig. 3.

In [20], dimensions of a printed triangular monopole antenna are computed using the design Equation (1). This design equation gives the triangle height (L) and side length (T) for selected -10 dB reflection coefficient lower cut-off frequency (f_L).

$$f_L = \frac{7.2 \text{ GHz}}{\{(L + r + p) \times k\}} \quad (1)$$

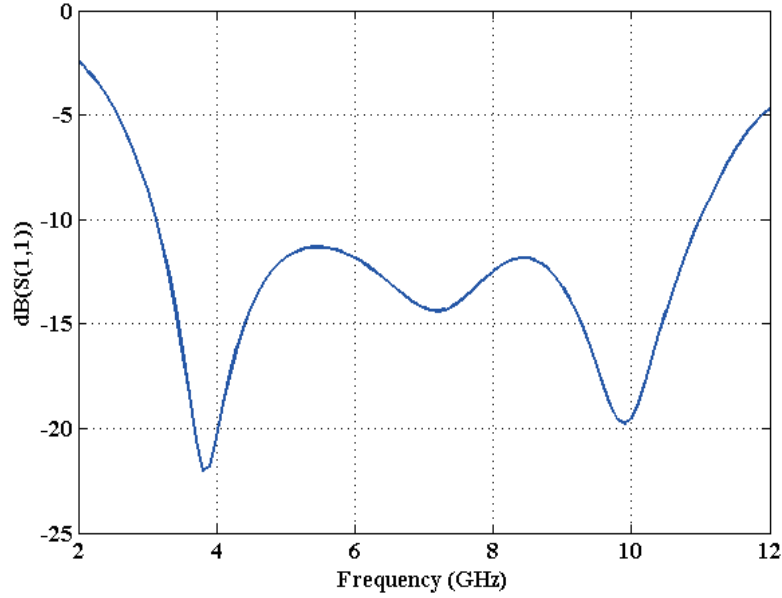


Figure 2. Simulated reflection coefficient curve of the proposed UWB antenna.

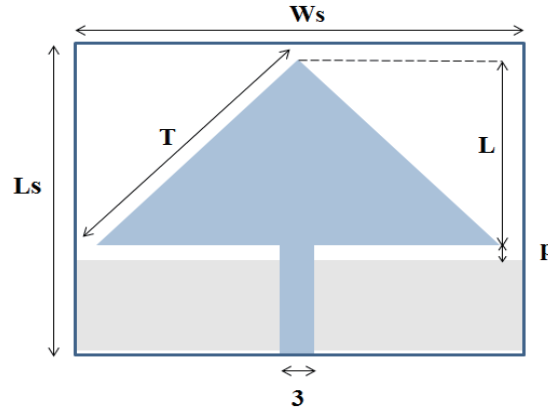


Figure 3. Printed triangular monopole antenna (PTMA) [20].

where,

$$L = \frac{\sqrt{3}T}{2} \quad \text{and} \quad r = \frac{T}{4\pi}$$

To achieve the -10 dB lower cut-off (f_L) of 3.1 GHz, the assumed frequency is 4 GHz, and an initial structure is designed as per mathematical relations. Then, the triangular structure is modified as reported in this paper to increase the side length that shifts the lower cut-off frequency from 4 GHz to around 3.1 GHz. This step objective is to shift the lower cut-off frequency towards left side as well as to reduce the triangular patch area. The considered -10 dB reflection coefficient lower cut-off frequency (f_L) is 4 GHz; feed gap (p) is 0.05 cm; and $k = 1.15$, which is constant [20]. Equation (1) can be modified in terms of side length as shown in Equation (2).

$$T = \frac{6.621}{f_L} - 0.05287 \quad (2)$$

From Equation (2), side length (T) of the triangle is obtained as 1.6 cm. Calculated triangle height (L) is 1.39 cm. Assumed length and width of the feed line are 0.35 cm and 0.25 cm, respectively for compact

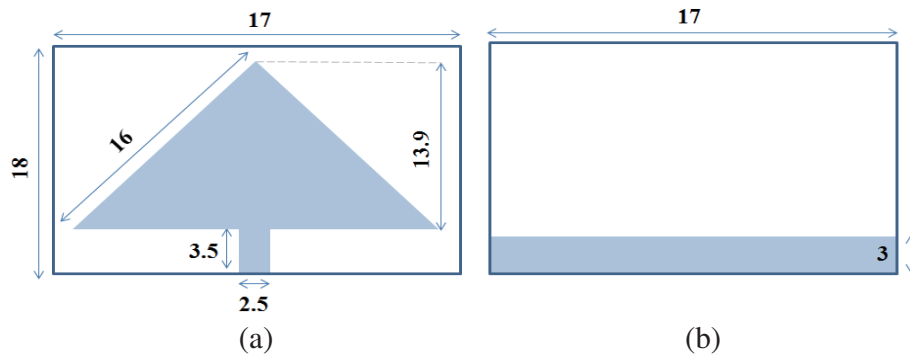


Figure 4. Planar triangular monopole antenna. (a) Top view. (b) Bottom view [All dimensions are in mm].

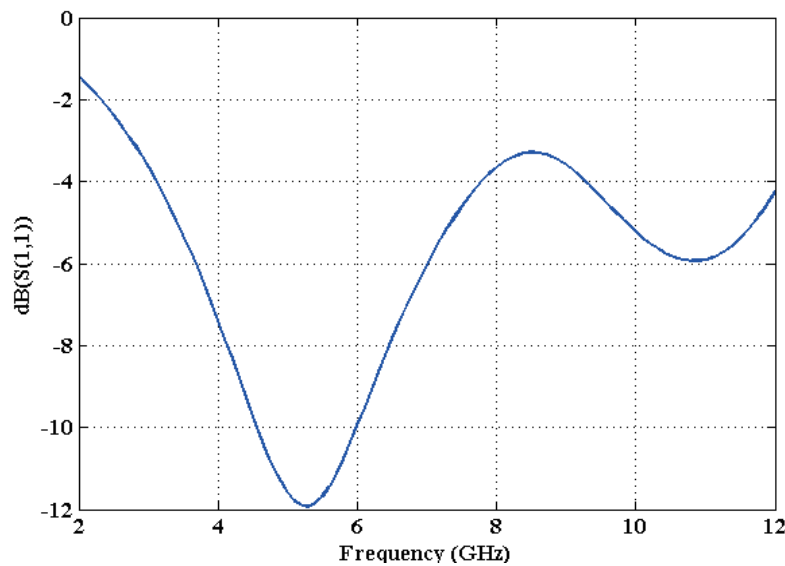


Figure 5. Simulated reflection coefficient curve of PTMA.

dimensions as well as for better impedance matching. The minimum substrate dimensions are found to be $18 \text{ mm} \times 17 \text{ mm}$ to cover the complete radiating patch as shown in Fig. 4. The simulated reflection coefficient plot of the planar triangular antenna is shown in Fig. 5.

From Fig. 5 it can be found that the -10 dB reflection coefficient lower cut-off frequency is found to be equal to 4.53 GHz . However, the required band 3.1 GHz to 10.6 GHz is not covered, and the -10 dB reflection coefficient lower cut-off frequency is 4.53 GHz . So, to obtain the lower cut-off near 3.1 GHz the triangular radiating patch is modified as shown in Fig. 6.

It is noted here that the height (L) of radiating patch is 13.9 mm , which is the same as the triangular patch, but only the side length is changed. Remaining dimensions like feed width, length, and partial ground are as per the initial design only. The increase in side length results in a shift of the -10 dB reflection coefficient lower cut-off frequency towards left side. Radius of the circular structures is adjusted in such a way that the -10 dB cut-off frequency appears around 3.1 GHz . Accordingly, optimized dimensions of the substrate are $18 \text{ mm} \times 12 \text{ mm}$. The corresponding antenna reflection coefficient curve is shown in Fig. 7.

From Fig. 7 it can be noticed that the -10 dB reflection coefficient lower cut-off frequency is around 3.1 GHz . It clearly means that by adopting the proposed structure the cut-off frequency is shifted from 4.53 GHz to around 3.1 GHz . However, the required UWB 3.1 GHz to 10.6 GHz is not yet covered. So, the required performance characteristics are obtained by following the further steps.

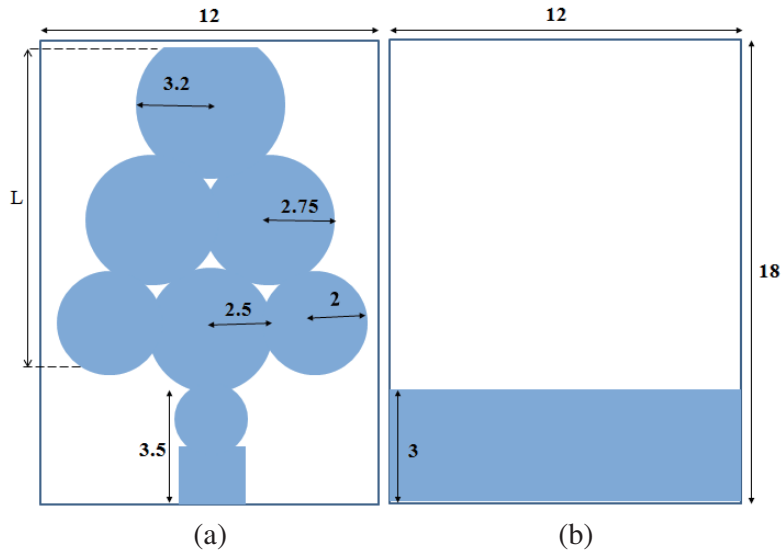


Figure 6. Proposed step UWB antenna. (a) Top view. (b) Bottom view.

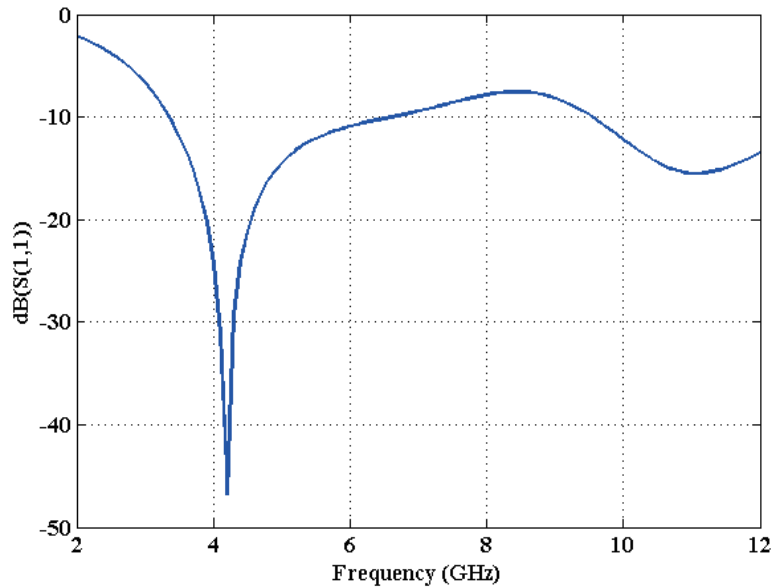


Figure 7. Simulated reflection coefficient curve.

3.2. Design Analysis of Ground Patch

In this antenna design, ground slots also play a major role to obtain the impedance matching over the complete UWB. The slots are also helpful in achieving a stable reflection coefficient performance. The design steps of the ground plane are shown in Fig. 8. Note that the radiating patch is the same for all the different ground planes.

Simulated reflection coefficient performance for the above-mentioned steps is shown in Fig. 9. From Fig. 9 it can be noted that the introduced ground slots are able to enhance the impedance matching in the required UWB. Moreover, it is also very clear that the slots are stabilizing the reflection coefficient performance, which can be observed from step 1 to proposed antenna reflection coefficient (S_{11}) curves [see Figs. 9(a), (b)]. In step 1, the antenna exhibits a sharp dip curve with dual band type

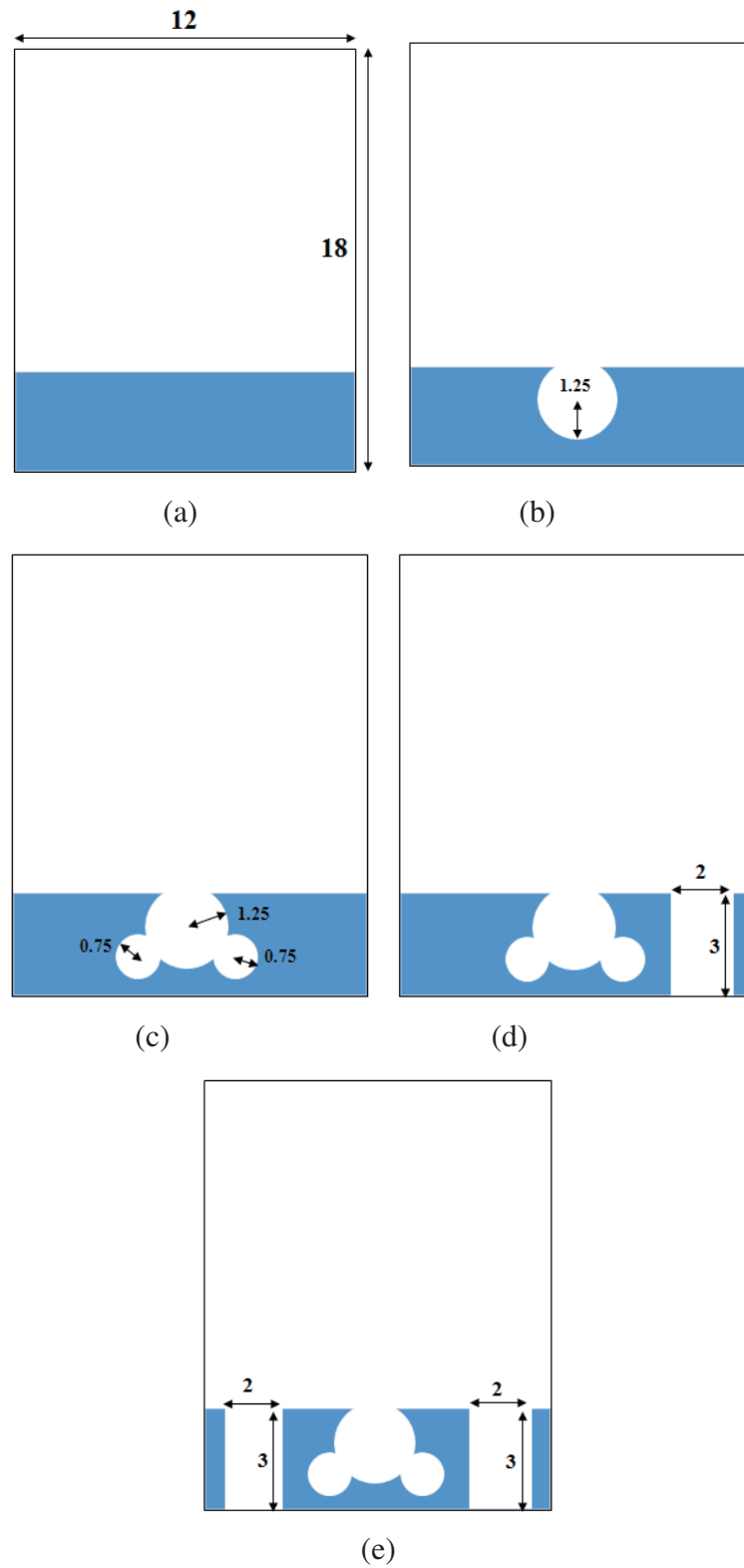
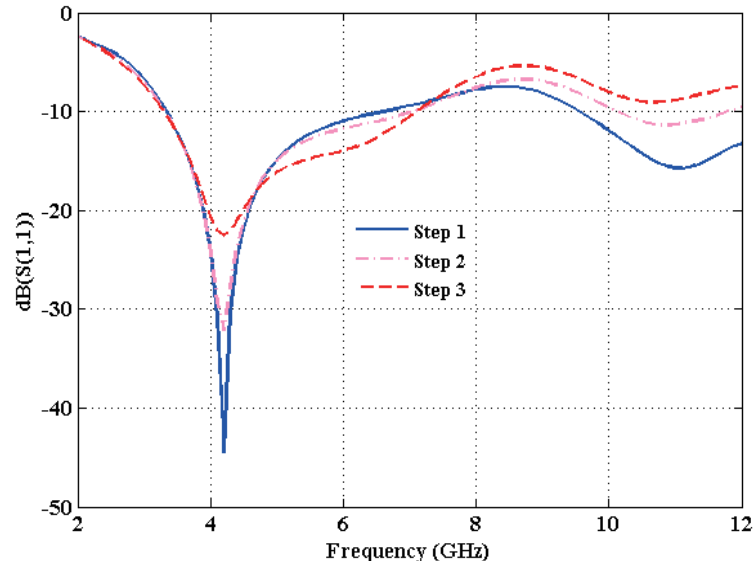
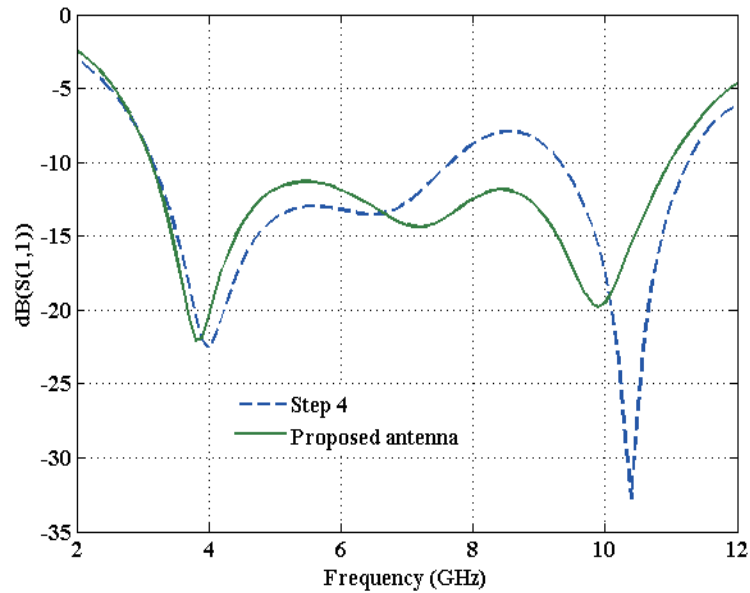


Figure 8. Design steps of ground plane. (a) Step 1. (b) Step 2. (c) Step 3. (d) Step 4. (e) Proposed antenna.



(a)



(b)

Figure 9. Simulated performance of reflection coefficient (S_{11}) for the mentioned steps (a) step 1 to step 3 (b) step 4 & proposed antenna.

performance as reported in Fig. 9(a). Then, in step 2, the sharp dip is smoothed, and the bandwidth in the lower band is slightly improved. However, the upper band performance is degraded due to the added ground slot. In step 3, the bandwidth in the lower band is also slightly improved, but the upper band performance is degraded due to added ground slots. From step 1 to step 3, it is very clear that the inserted slots are smoothing the reflection coefficient performance and also able to achieve a slight improvement in bandwidth at the lower band. As observed from Fig. 9(b), in step 4, the inserted rectangular ground slot adds one resonating frequency at 10.4 GHz. Then, by adding one more rectangular slot the complete bandwidth is enhanced, and the required UWB is obtained.

The effect of ground slots can also be understood from the surface current distribution as shown in Fig. 10. Surface current distribution on the proposed antenna at different frequencies is shown in

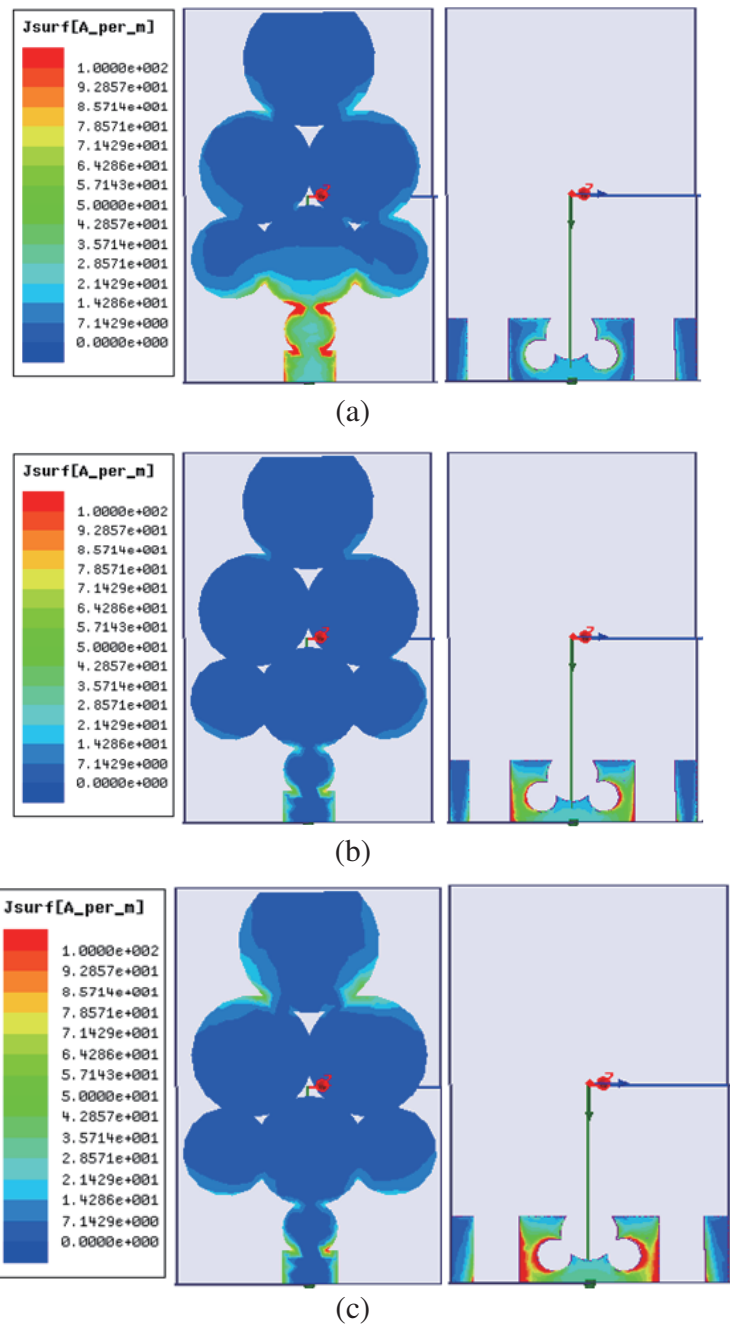


Figure 10. Surface current distribution on the proposed antenna at (a) 3.8 GHz (b) 9 GHz and (c) 9.9 GHz.

Fig. 10. From Fig. 10 it can be clearly inferred that strong surface currents reside in the ground plane at higher frequencies. This is because as mentioned earlier the ground rectangular slots are responsible for producing resonating frequencies at the higher operating band. From this observation it can also be confirmed that the rectangular slots on the ground plane produce a band at higher frequencies.

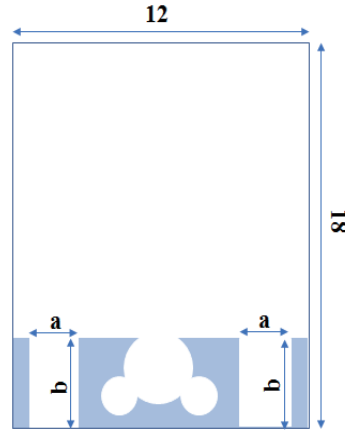
A comparison table presenting the performance parameters in the different steps is shown in Table 2. Note that the gain and radiation efficiency characteristics are found to be approximately the same for all the design steps. However, impedance bandwidth varies from one step to another. From Table 2 the conclusion points mentioned for the design steps can also be verified.

Table 2. Performance parameters in different steps.

Design step	-10 dB dB(S(1,1)) range	Impedance Bandwidth	Max. peak Gain	Min. radiation efficiency
Step 1	3.35–6.6 GHz and 9.6–12.8 GHz	3.25 GHz and 3.2 GHz	5.35 dBi at 9.5 GHz	94.75%
Step 2	3.3–7.1 and 10.15–11.8 GHz	3.8 GHz and 1.65 GHz	5.35 dBi at 9.5 GHz	94.75%
Step 3	3.3–7.25 GHz	3.95 GHz	5.35 dBi at 9.5 GHz	94.75%
Step 4	3.15–7.65 GHz and 9.3–11.35 GHz	4.5 GHz and 2.05 GHz	5.05 dBi at 9 GHz	94.5%
Proposed antenna	3.1–11 GHz	7.9 GHz	5.05 dBi at 9 GHz	94.5%

4. PARAMETRIC ANALYSIS

In this section, various parametric studies performed on the proposed antenna are reported. In this study, the effect of ground rectangular slots on the reflection coefficient is mainly observed. The rectangular slots width, length, and position from their current state are varied as presented in Fig. 11. The resulting parametric study performance characteristics are shown in Fig. 12. From Fig. 12 it can also be noted that the selected slot width, length, and positions are optimum to achieve maximum impedance bandwidth with $S_{11} \leq -10$ dB in the UWB range. In remaining cases, the performance is either degrading or not stable.

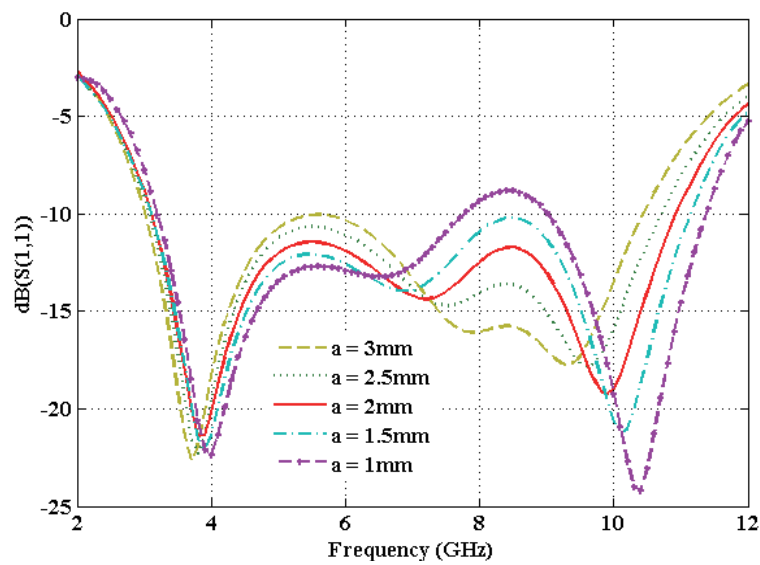
**Figure 11.** Proposed antenna ground layer presenting the parametric study variables.

5. RESULTS AND DISCUSSION

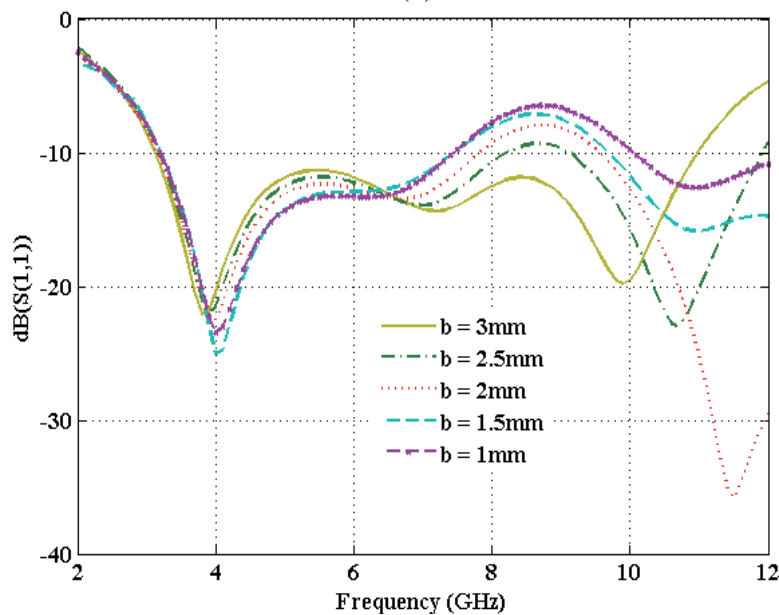
This section mainly focuses on the fabrication and discussion of the measurement results. To justify and validate the simulation results, the prototype of the proposed compact UWB antenna is printed on a cost-effective FR-4 substrate. The fabricated prototype of the proposed antenna design is shown in Fig. 13(a). This fabricated antenna model has been experimentally tested using Anritsu MS2037C analyzer as shown in Fig. 13(b) to assure its UWB operation with a very attractive size of 18×12 mm².

The comparison of simulation & measurement reflection coefficient performances is shown in Fig. 14. As per measurement results, the antenna offers an impedance-bandwidth of 8.1 GHz (3.1–11.2 GHz) which is in good agreement with the simulated results, verifying the conceptual approach of the suggested antenna. The simulated and measured peak gains of the UWB antenna are shown in Fig. 15. From Fig. 15 it is noted that the maximum peak-gain is found to be 5.05 dBi at 9 GHz. The simulated 3D-radiation pattern at 9 GHz is shown in Fig. 16.

From Fig. 16 it can also be confirmed that the peak gain at 9 GHz is 5.05 dBi. It is also noted From Fig. 16 that the radiation pattern has a slight directional behavior. The radiation patterns of the proposed array antenna are measured with the support of a driving software system using a turntable mechanism setup. At the transmitting end, a standard gain horn antenna is used which is excited with a microwave signal generator, and the antenna under test (proposed antenna) is placed at the receiving side. By rotating AUT, the radiation patterns are measured. Based on the recorded measured values, the measured radiation patterns are obtained and compared with the simulated ones for the



(a)



(b)

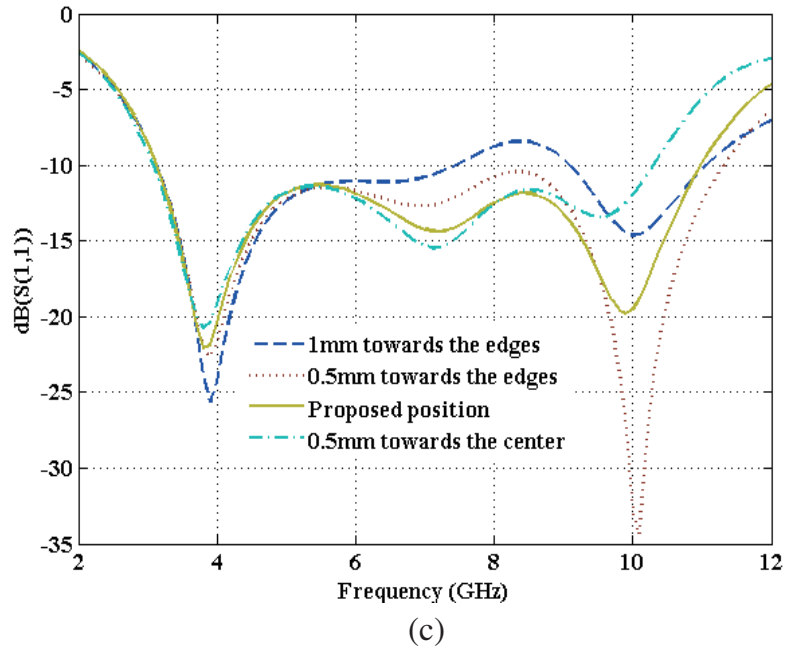
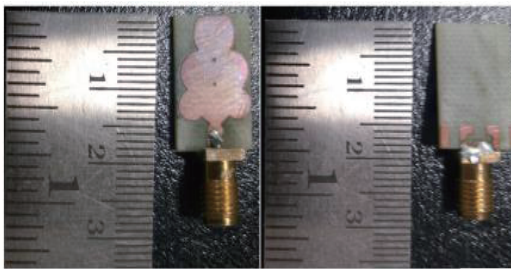
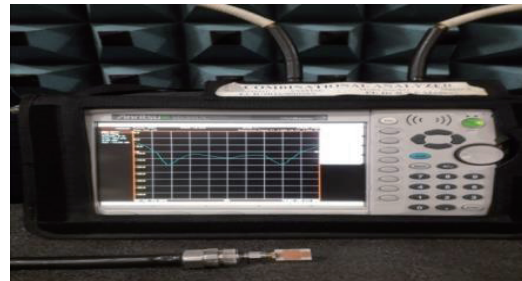


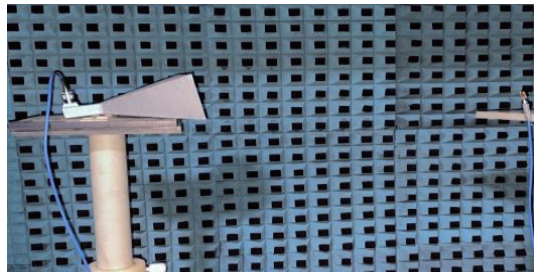
Figure 12. Reflection coefficient (S_{11}) performance for variation in (a) slot width, (b) slot length, (c) slot position from its current position.



(a)



(b)



(c)

Figure 13. Experiment details, (a) fabricated prototype, (b) VNA set up, (c) anechoic chamber view.

frequencies 3.8 GHz, 9 GHz, and 9.9 GHz as shown in Fig. 17. It shows radiation pattern for both the phases, i.e., for $\phi = 0^\circ$ and $\phi = 90^\circ$. From Fig. 17 it can be noted that the radiation pattern is omnidirectional at the lower frequency but slightly directional at higher operating frequencies. This is mainly due to the antenna structure and decrement in wavelength as frequency increases. The simulated and measured radiation efficiencies over the operating range are shown in Fig. 18. Fig. 18 depicts that a minimum radiation efficiency of 94.5% is found in the entire operating UWB. Also, at lower frequencies

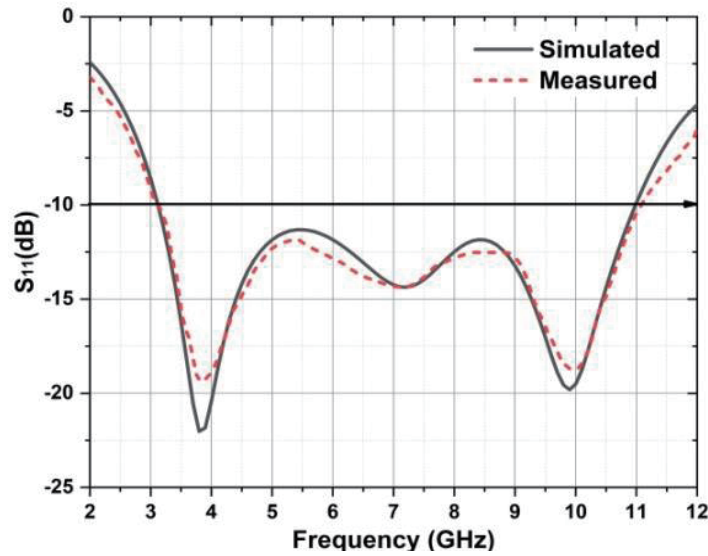


Figure 14. Comparison of simulation and measurement reflection coefficient performance.

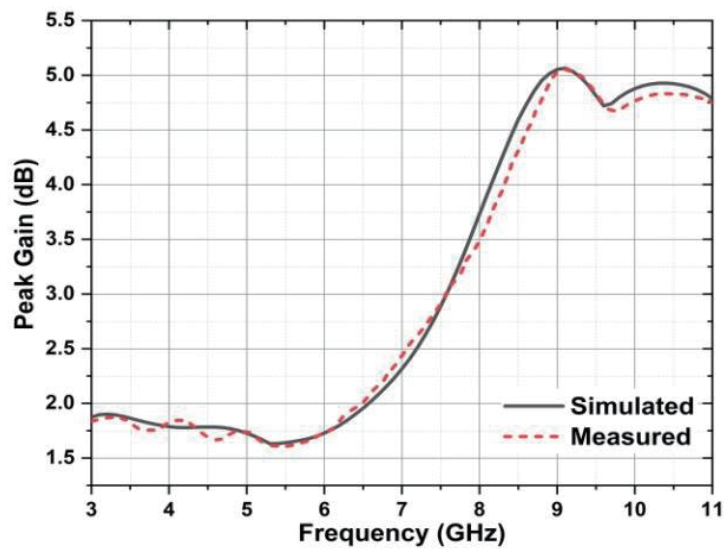


Figure 15. Peak gain plots of the UWB antenna.

Table 3. Simulated and measured performances.

Parameter	Simulation	Measurement
-10 dB dB(S(1,1)) range	3.1–11 GHz	3.1–11.2 GHz
Impedance Bandwidth	7.9 GHz	8.1 GHz
Max. Peak Gain (dBi)	5.05 dBi at 9 GHz	5 dBi at 9 GHz
Radiation efficiency	94.5%	94.35%

the radiation efficiency is high, and it decreases as frequency increases. The face to face and side to side group delay performances of the proposed antenna are shown in Fig. 19. The transmitting and receiving antennas are separated by a distance of 30 cm, and the face to face, side by side group delays

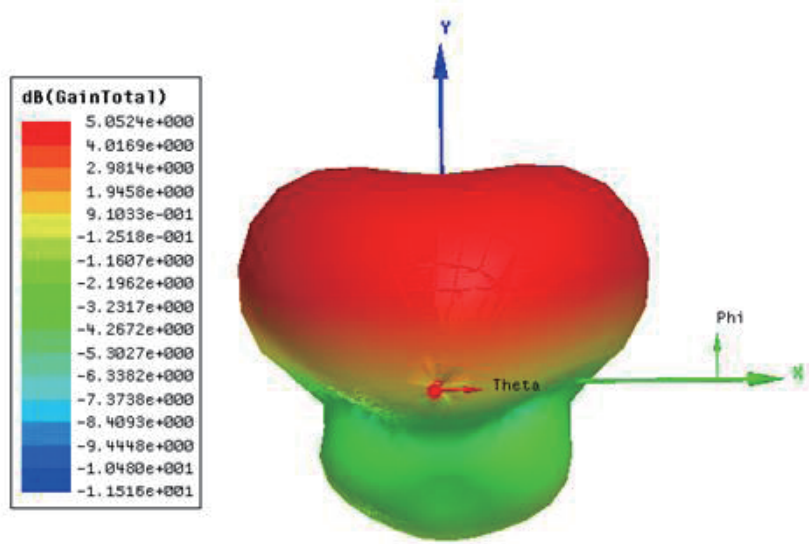
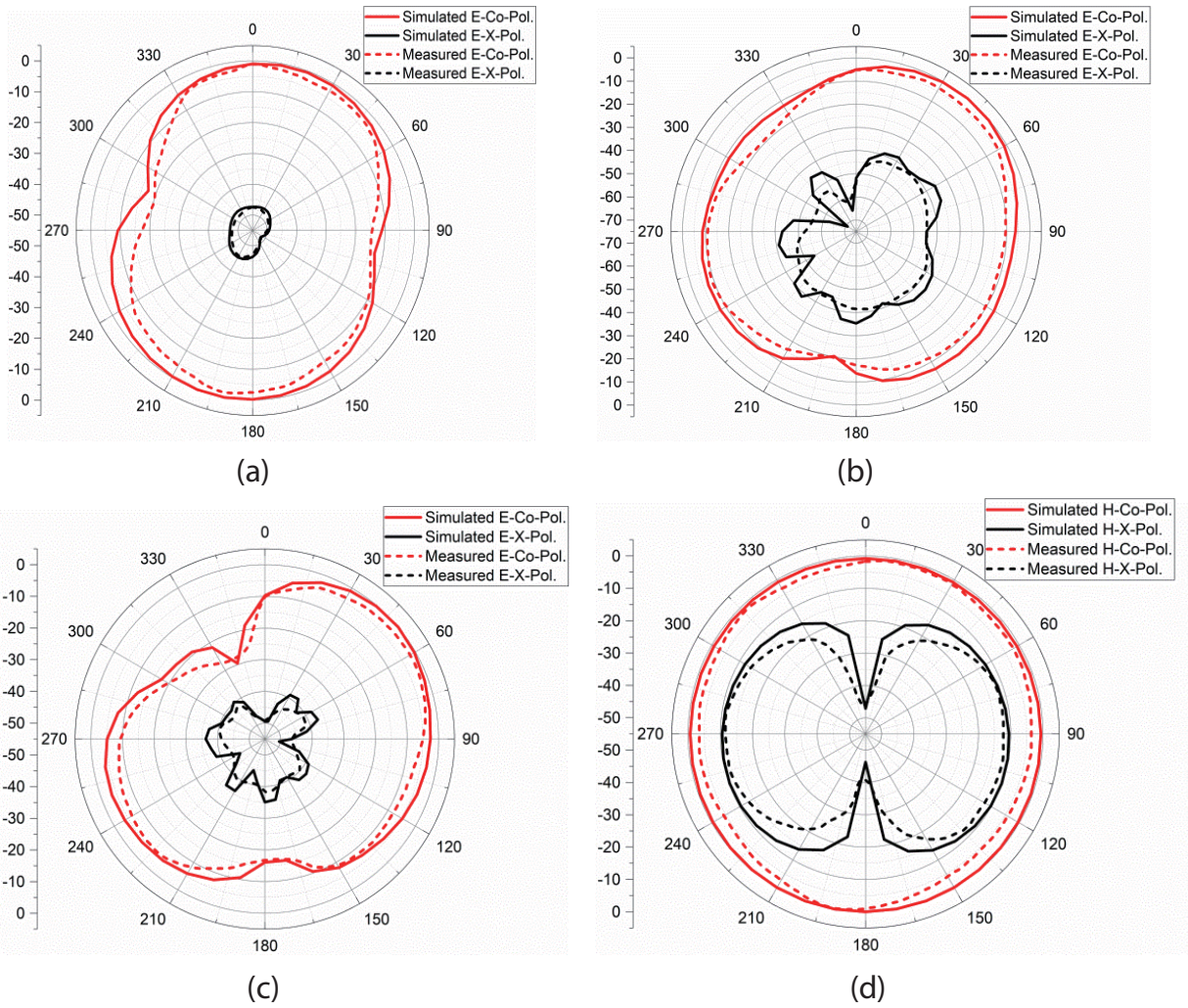


Figure 16. Simulated 3D-radiation pattern at 9 GHz.



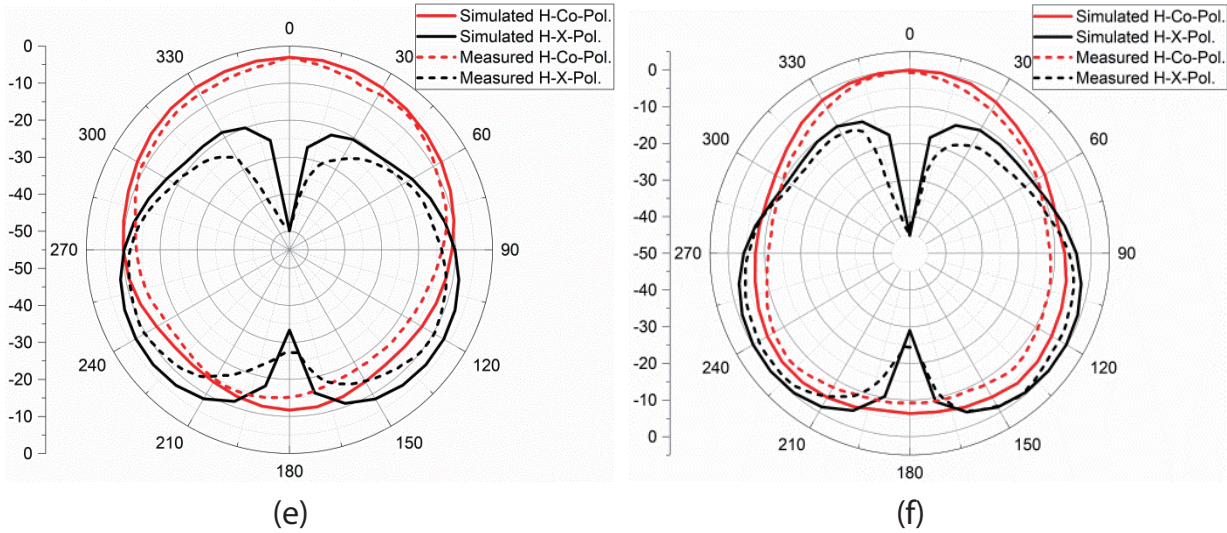


Figure 17. 2D radiation patterns E -plane at (a) 3.8 GHz, (b) 9 GHz, (c) 9.9 GHz, and H -plane at (d) 3.8 GHz (e) 9 GHz and (f) 9.9 GHz.

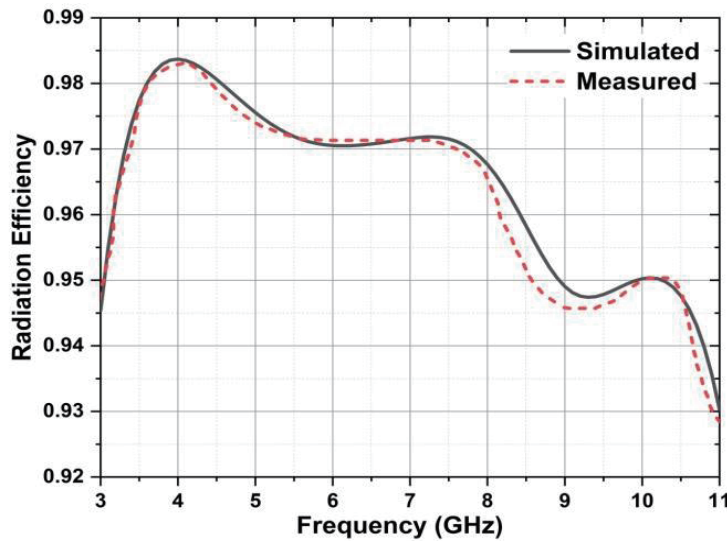


Figure 18. Radiation efficiency over the UWB.

are tested. From Fig. 19 it is very clear that the proposed antenna has a stable group delay performance in the entire operating band with a maximum group delay of 1.48 ns for the face-to-face case, while the side-by-side case has a maximum group delay of 0.315 ns which indicates desired time-domain behavior of the antenna and confirms its suitability for UWB communications. A comparison table that shows simulated and measured performances is presented in Table 3.

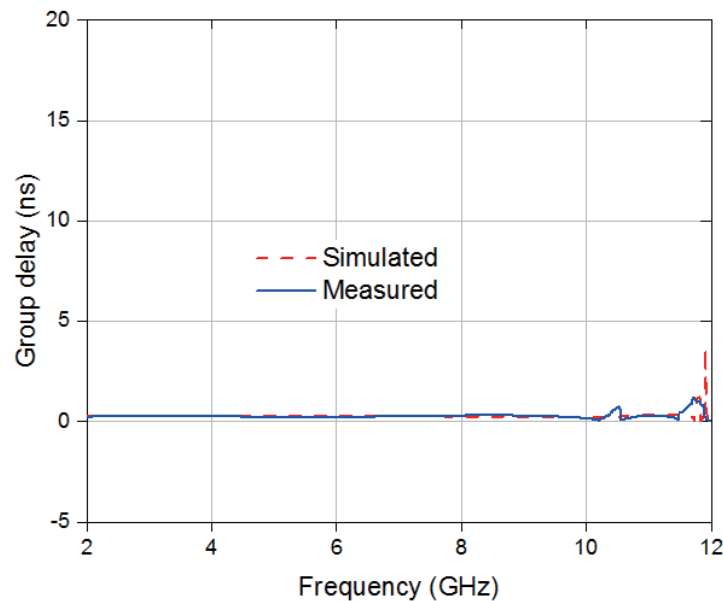
Table 3 infers that the simulated & measured results are in good agreement. The suggested UWB antenna is compared with other conventional type antenna structures reported in the literature for UWB applications, and the comparison summary is included in Table 4.

It is observed from Table 4 that the dimension of the proposed antenna is the smallest. The proposed novel configured antenna occupies a much smaller area to support UWB communication and also offers better gain characteristics than the other reported works. It can also be found that the antenna results in better time domain and frequency domain characteristics. Moreover, the structure and design techniques are very novel.

Table 4. Comparison table.

Ref.	Dimensions (mm ³)	Bandwidth (GHz)	Max. Peak Gain (dBi)	Rad. Efficiency (%)	Group delay (ns)
[2]	24 × 28 × 0.787	2.76–12.8	5.3	-	-
[3]	25 × 25 × 1.6	2.6–13.04	4.25	-	1
[4]	25 × 25 × 0.8	3.01–11.3	6.1	-	2
[5]	25 × 20 × 1.6	3.1–10.64	4.34	Max. 96.77	-
[6]	30 × 51 × 1.6	3–12.6	3	-	-
[8]	35 × 35 × 1.6	3.1–12	4.5	-	-
[9]	35 × 30 × 1.6	3.2–12	4.85	-	0.52
[12]	28 × 29 × 1.6	3.8–12	4.5	-	0.4
[13]	25 × 17 × 1.6	2.94–22.2	5.18	Min. 70	±2
[14]	24 × 16 × 0.8	3.1–10.7	-	-	-
[15]	16 × 21 × 1.6	3.77–11.64	4.32	Min. 85.69	1.36
[16]	18.7 × 17.6 × 1.5	2.9–13.7	Avg. 4.4	-	-
[17]	12 × 19 × 1.6	2.9–12	3.18	Max. 95	2
*	18 × 12 × 1.6	3.1–11	5.05	Min. 94.35 Max. 98.25	1.48

* Proposed work



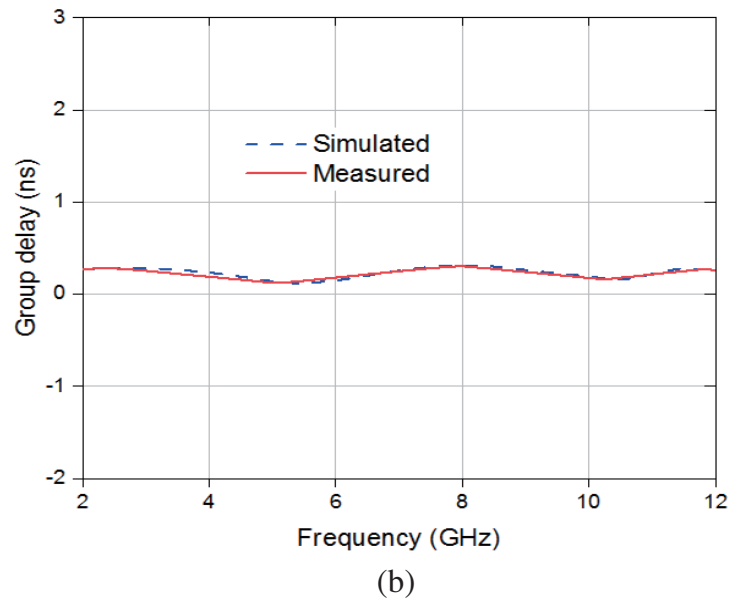


Figure 19. Group delay performance. (a) Face-face. (b) Side by side antenna positions.

6. CONCLUSION

This study discusses an $18\text{ mm} \times 12\text{ mm} \times 1.6\text{ mm}$ planar ultra-wide band antenna performance-characteristics for unlicensed-frequency range applications in the band 3.1–10.6 GHz. This antenna has achieved a reflection-coefficient of $\leq -10\text{ dB}$ in the UWB 3.1–11 GHz frequency range. The antenna is able to achieve the maximum peak-gain of 5.05 dBi at 9 GHz and a minimum radiation efficiency of 94.5% in the entire operating band. The results of fabricated prototype are verified, and a good agreement is noted. Because of small size, good time domain, and frequency domain performance, the proposed antenna is an appropriate module for various unlicensed-frequency range UWB applications like W-BAN, W-LAN, CR spectrum sensing, wireless sensor networks, etc.

REFERENCES

1. FCC 1st report and order on Ultra-Wideband Technology, Feb. 2002.
2. Koohestani, M. and M. Golpour, "U-shaped microstrip patch antenna with novel parasitic tuning stubs for ultra-wideband applications," *IET Microwaves, Antennas & Propagation*, Vol. 4, No. 7, 938–946, 2010.
3. Gautam, A. K., S. Yadav, and B. K. Kanaujia, "A CPW-fed compact UWB microstrip antenna," *IEEE Antennas and Wireless Propagation Letters*, Vol. 12, 151–154, 2013.
4. Song, K., Y.-Z. Yin, S.-T. Fan, and B. Chen, "Compact open-ended L-shaped slot antenna with asymmetrical rectangular patch for UWB applications," *Progress In Electromagnetics Research*, Vol. 19, 235–243, 2011.
5. Ravi, K. T., S. Warathe, and N. Anveshkumar, "Design of a circular planar UWB antenna and its higher cut-off frequency enhancement," *In Proceedings of the IEEE 10th International Conference on Computing, Communication and Networking Technologies (ICCCNT)*, 1–6, Kanpur, India, Jul. 2019.
6. Prombutr, N., P. Kirawanich, and P. Akkaraekthalin, "Bandwidth enhancement of UWB microstrip antenna with a modified ground plane," *International Journal of Microwave Science and Technology*, 2009.

7. Naser Moghadasi, M., R. Sadeghi Fakhr, and A. Danideh., "CPW-fed compact slot antenna for WLAN operation in a laptop computer," *Microwave and Optical Technology Letters*, Vol. 52, No. 6, 1280–1282, 2010.
8. Ali, W. A., H. A. Mohamed, A. A. Ibrahim, and M. Z. Hamdalla, "Gain improvement of tunable band-notched UWB antenna using metamaterial lens for high speed wireless communications," *Microsystem Technologies*, Vol. 25, No. 11, 4111–4117, 2019.
9. Choi, S. H., J. K. Park, S. K. Kim, and J. Y. Park, "A new ultra-wideband antenna for UWB applications," *Microwave and Optical Technology Letters*, Vol. 40, No. 5, 399–401, 2004.
10. Nella, A. and A. S. Gandhi, "Moon slotted circular planar monopole UWB antenna design and analysis," *Proceedings of the IEEE 6th International Conference on Advances in Computing, Communications and Informatics (ICACCI)*, Manipal, Karnataka, India, 595-600, Sept. 2017.
11. Anvesh Kumar, N. and A. S. Gandhi, "Small size planar monopole antenna for high speed UWB applications," *Proceedings of the 22nd National Conference on Communication (NCC)*, 1–5, Guwahati, Assam, India, Mar. 2016.
12. Kasi, B., L. C. Ping, and C. K. Chakrabarty, "A compact microstrip antenna for ultra-wideband applications," *European Journal of Scientific Research*, Vol. 67, No. 1, 45–51, 2011.
13. Tiwari, R. N., P. Singh, and B. K. Kanaujia, "A modified microstrip line fed compact UWB antenna for WiMAX/ISM/WLAN and wireless communications," *AEU-International Journal of Electronics and Communications*, Vol. 104, 58–65, 2019.
14. Ebadzadeh, S. R., et al., "A compact UWB monopole antenna with rejected WLAN band using split-ring resonator and assessed by analytic hierarchy process method," *Journal of Microwaves, Optoelectronics and Electromagnetic Applications*, Vol. 16, 592–601, 2017.
15. Devana, V. N., et al., "A novel compact fractal UWB antenna with dual band notched characteristics," *Analog Integrated Circuits and Signal Processing*, Vol. 110, No. 2, 349–360, 2022.
16. Syed, A. and R. W. Aldhaheeri. "A very compact and low profile UWB planar antenna with WLAN band rejection," *The Scientific World Journal*, 2016.
17. Doddipalli, S. and A. Kothari, "Compact UWB antenna with integrated triple notch bands for WBAN applications," *IEEE Access*, Vol. 7, 183–190, 2018.
18. Rao, G. S., S. S. Kumar, and R. Pillalamarri, "Cross shaped slot printed UWB monopole antenna with notch function," *Microsystem Technologies*, Vol. 21, No. 11, 2327–2330, 2015.
19. Gayatri, T., N. Anveshkumar, and V. K. Sharma, "A hexagon slotted circular monopole UWB antenna for cognitive radio applications," *2020 International Conference on Emerging Trends in Information Technology and Engineering (ic-ETITE)*, 1–5, IEEE, 2020.
20. Ray, K. P., "Design aspects of printed monopole antennas for ultra-wide band applications," *International Journal of Antennas and Propagation*, Vol. 2008, Article ID: 713858, 8 pages, 2008.
21. Rahman, M., et al., "Compact UWB band-notched antenna with integrated bluetooth for personal wireless communication and UWB applications," *Electronics*, Vol. 8, No. 2, 158, 2019.
22. Rahman, M., D.-S. Ko, and J.-D. Park, "A compact multiple notched ultra-wide band antenna with an analysis of the CSRR-TO-CSRR coupling for portable UWB applications," *Sensors*, Vol. 17, No. 10, 2174, 2017.
23. Elajoumi, S., A. Tajmouati, J. Zbitou, A. Errkik, A. M. Sanchez, and M. Latrach, "Bandwidth enhancement of compact microstrip rectangular antennas for UWB applications," *Telkomnika*, Vol. 17, No. 3, 1559–1568, 2019.
24. El Hamdouni, A., A. Tajmouati, J. Zbitou, H. Bennis, A. Errkik, L. El Abdellaoui, and M. Latrach, "A low cost fractal CPW fed antenna for UWB applications with a circular radiating patch," *Telkomnika*, Vol. 18, No. 1, 436–440, 2020.